FIGURE S1

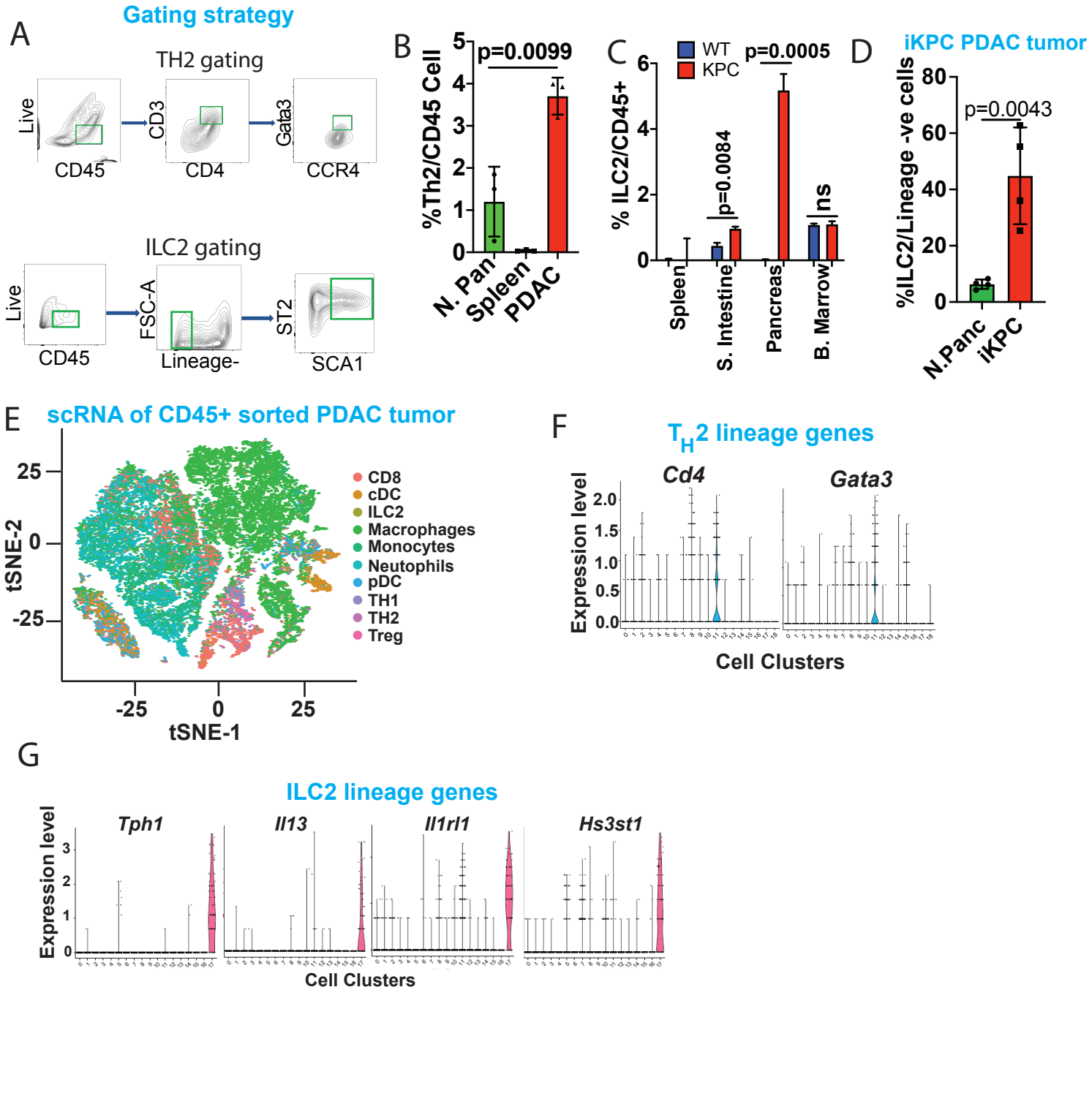
A
Gating strategy
TH2 gating
Live
CD45
CD3
CD4
Gata3
CCR4
ILC2 gating
Live
CD45
FSC-A
Lineage-
ST2
SCA1
B
%Th2/CD45 Cell
p=0.0099
N. Pan
Spleen
PDAC
C
WT
KPC
p=0.0005
% ILC2/CD45+
p=0.0084
ns
Spleen
S. Intestine
Pancreas
B. Marrow
D
iKPC PDAC tumor
%ILC2/Lineage -ve cells
p=0.0043
N.Panc
iKPC
E
scRNA of CD45+ sorted PDAC tumor
tSNE-2
tSNE-1
CD8
cDC
ILC2
Macrophages
Monocytes
Neutophils
pDC
TH1
TH2
Treg
F
TH2 lineage genes
Cd4
Gata3
Expression level
Cell Clusters
G
ILC2 lineage genes
Tph1
Il13
Il1rl1
Hs3st1
Expression level
Cell Clusters

Figure S1: Type 2 immune cell infiltration in PDAC tumors. Related to Figure 1.

(A) Gating strategy of T_H2 (top), and ILC2 (bottom).

(B) Frequency of T_H2 cells out of total $CD4^+$ cells in shCtrl vs shIL33 orthotopic PDAC tumor. T_H2 cells are $Gata3^+Foxp3^-$.

(C) Frequency of ILC2 cells out of total $CD45^+$ cells in spleen, small intestine, pancreas and bone marrow (n=3) in KPC mice compared to control C57BL/6 (WT) mice.

(D) Frequency of ILC2 cells out of total Lin^- cells in normal pancreas (n=3) compared to PDAC (n=4) in iKPC mice.

(E) tSNE plots showing immune cell clusters from scRNAseq dataset of iKPC (AK-B6 cell line) transplanted tumor.

(F) Violin plot showing expression of T_H2 lineage genes *Cd4* and *Gata3*.

(G) Violin plot showing expression of ILC2 lineage genes *Tph1, Il13, Il1rl1*, and *Hs3st1*. Results are shown as mean ±SD. p-values were calculated using Student t-test. Individual p-values are indicated in the figures.

FIGURE S2

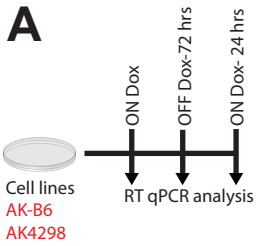

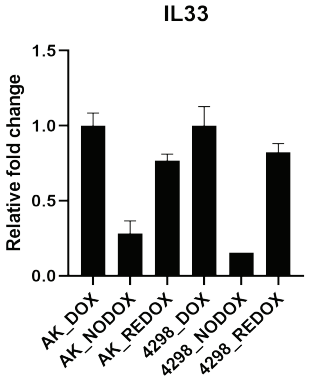

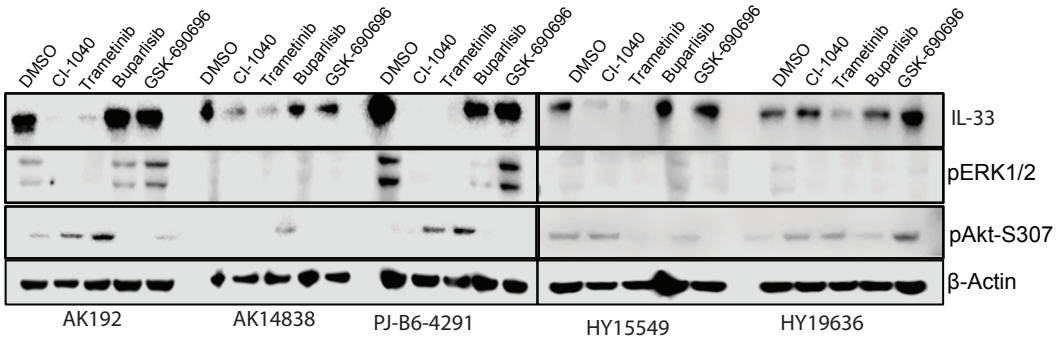

D

Expression * Group Crosstabulation

Count

		Group		
		Normal	Tumor	Total
Expression	Negative	37	3	40
	Low	21	23	44
	Medium	5	49	54
	High	0	18	18
Total		63	93	156

Chi-Square Tests

	Value	df	Asymp. Sig. (2-sided)
Pearson Chi-Square	80.033[a]	3	.000
Likelihood Ratio	94.922	3	.000
Linear-by-Linear Association	74.960	1	.000
N of Valid Cases	156		

a. 0 cells (0.0%) have expected count less than 5. The minimum expected count is 7.27.

Correlations

			N	T
Spearman's rho	N	Correlation Coefficient	1.000	.711**
		Sig. (2-tailed)		.000
		N	53	53
	T	Correlation Coefficient	.711**	1.000
		Sig. (2-tailed)	.000	
		N	53	93

E

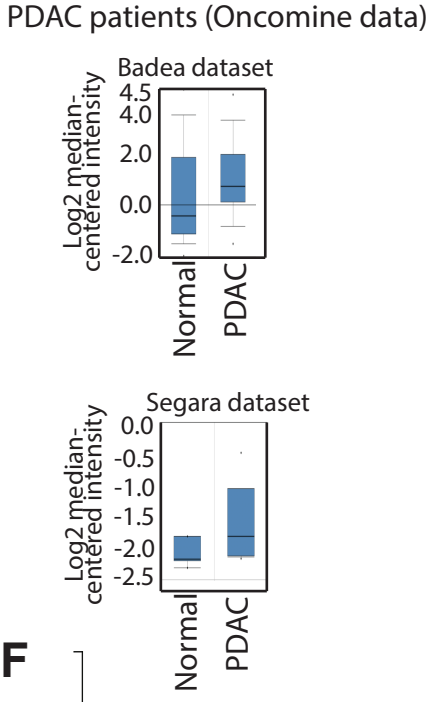

F

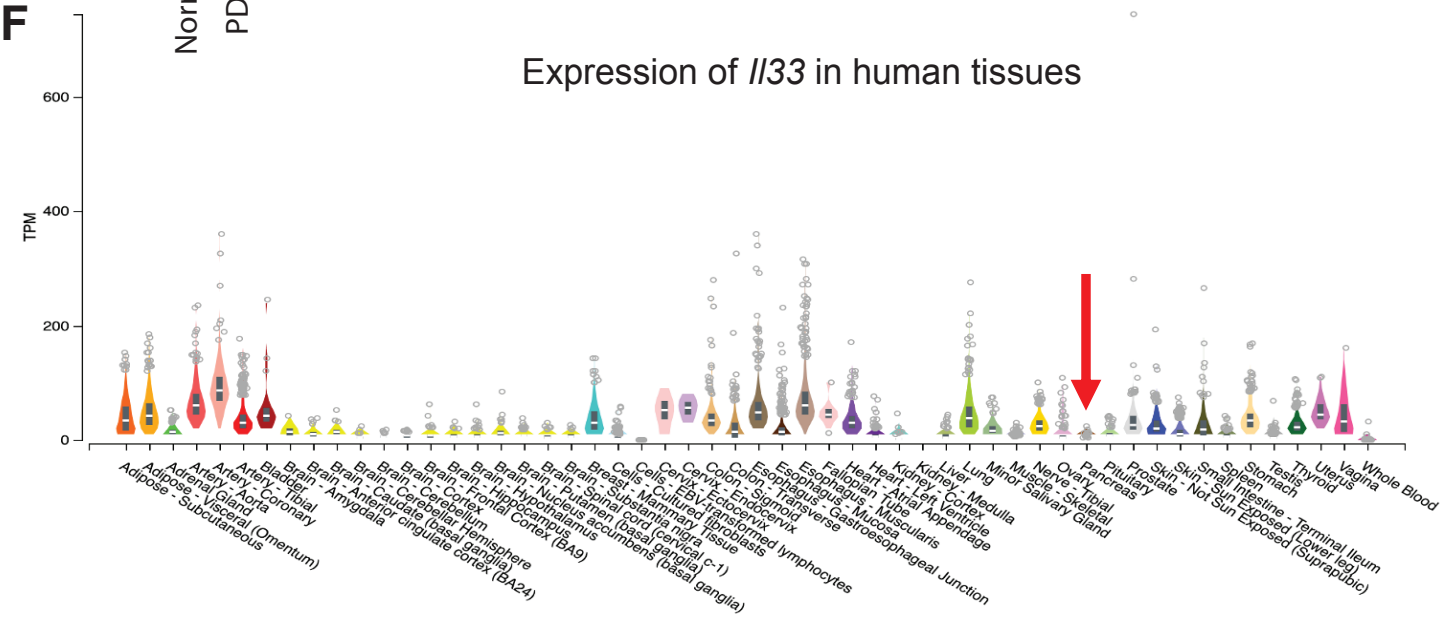

Figure S2: $Kras^{G12D}$ drives IL-33 expression in PDAC. Related to Figure 2.

(A) Schematic showing strategy for doxycycline (dox) inducible iKPC cell line AK-B6 and AK4298 for RT-qPCR analysis.

(B) RT-qPCR analysis of *Il33* in AK-B6 and AK4298 cell line after KRAS ON and OFF conditions (n=3).

(C) Western blot analysis of IL-33, pERK1/2, pAkt-S307 upon treatment with MEK (CI1040 and Trametinib) and AKT (Buparlisib and GSK-690696) inhibitors for 24 hrs in different PDAC mouse cell lines. β-actin was used as a loading control.

(D) Tables for human PDAC TMA analysis showing IL-33 expression profile and statistical analysis of adjacent normal (n=63) vs PDAC tumor (n=93).

(E) Plots showing Oncomine dataset analysis for *Il33* expression in normal vs PDAC tumors.

(F) Representative plot showing *Il33* expression profile in normal human tissues (GTEx: Genotype tissue expression).

Results are shown as mean ±SD. p-values were calculated using Student t-test. Chi-square test and spearman's correlation analysis was done for human PDAC TMA for statistical significance. Individual p-values are indicated in the figures.

FIGURE S3

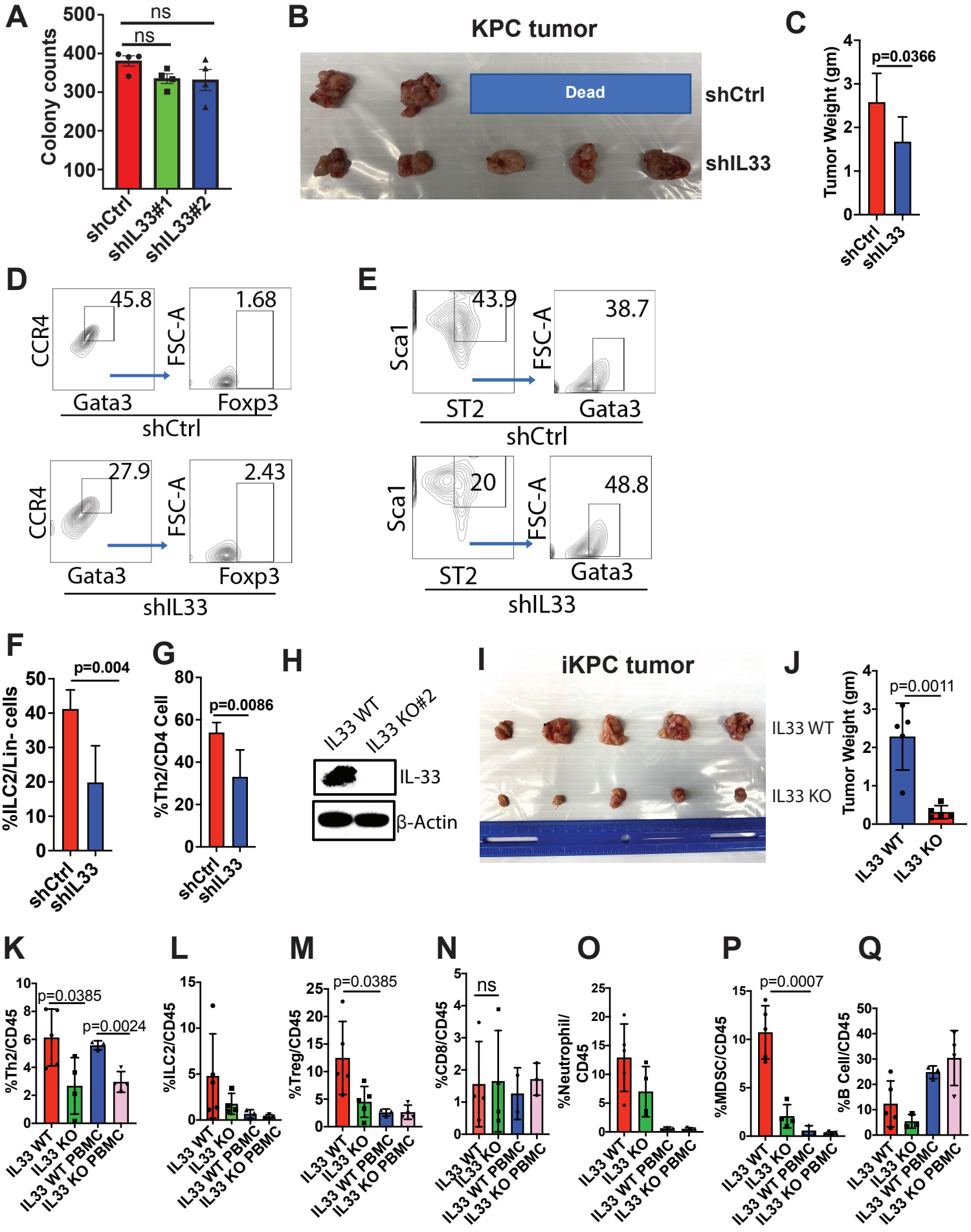
A
Colony counts
500
400
300
200
100
ns
ns
shCtrl
shIL33#1
shIL33#2
B
KPC tumor
Dead
shCtrl
shIL33
C
Tumor Weight (gm)
p=0.0366
shCtrl
shIL33
D
45.8
CCR4
FSC-A
1.68
Gata3
Foxp3
shCtrl
27.9
CCR4
FSC-A
2.43
Gata3
Foxp3
shIL33
E
43.9
Sca1
FSC-A
38.7
ST2
Gata3
shCtrl
20
Sca1
FSC-A
48.8
ST2
Gata3
shIL33
F
%ILC2/Lin- cells
p=0.004
shCtrl
shIL33
G
%Th2/CD4 Cell
p=0.0086
shCtrl
shIL33
H
IL33 WT
IL33 KO#2
IL-33
β-Actin
I
iKPC tumor
IL33 WT
IL33 KO
J
Tumor Weight (gm)
p=0.0011
IL33 WT
IL33 KO
K
%Th2/CD45
p=0.0385
p=0.0024
IL33 WT
IL33 KO
IL33 WT PBMC
IL33 KO PBMC
L
%ILC2/CD45
IL33 WT
IL33 KO
IL33 WT PBMC
IL33 KO PBMC
M
%Treg/CD45
p=0.0385
IL33 WT
IL33 KO
IL33 WT PBMC
IL33 KO PBMC
N
%CD8/CD45
ns
IL33 WT
IL33 KO
IL33 WT PBMC
IL33 KO PBMC
O
%Neutrophil/ CD45
IL33 WT
IL33 KO
IL33 WT PBMC
IL33 KO PBMC
P
%MDSC/CD45
p=0.0007
IL33 WT
IL33 KO
IL33 WT PBMC
IL33 KO PBMC
Q
%B Cell/CD45
IL33 WT
IL33 KO
IL33 WT PBMC
IL33 KO PBMC

Figure S3: **IL-33 depletion delays tumor progression. Related to Figure 3.**

(A) Colony formation assay of shCtrl and shIL33 stable iKPC cell line. Cells were fixed and stained with crystal violet and colonies were quantified using ImageJ (n=4).

(B) (Top) Western blot showing shRNA knockdown of IL-33 in KPC cell line. (Bottom) Representative images of orthotopic transplanted shCtrl and shIL33 KPC pancreatic tumors (n=5). Three mice died of tumor burden prior to the termination of the experiment.

(C) Bar graph showing tumor weight of shCtrl and shIL33 orthotopically transplanted KPC pancreatic tumors (n=5).

(D) Flow cytometric plots of T_H2 cells out of total $CD4^+$ cells in shCtrl vs shIL33 orthotopic PDAC tumor. T_H2 cells are $CD45^+CCR4^+Gata3^+Foxp3^-$.

(E) Flow cytometric plots of ILC2 out of total Lin^- cells in shCtrl vs shIL33 orthotopic PDAC tumor. ILC2 cells are $CD45^+Lin^-Sca1^+ST2^+Gata3^+$.

(F) Frequency of ILC2s in orthotopic transplanted shCtrl and shIL33 in KPC tumors relative to total Lin^- cells.

(G) Frequency of T_H2 in orthotopic transplanted shCtrl and shIL33 in KPC tumors relative to total $CD4^+$ cells.

(H) Western blot analysis of IL33 WT and IL33 KO PDAC cells. β-actin was used as a loading control.

(I) Representative images of orthotopically transplanted IL33 WT and IL33 KO PDAC tumors (n=5).

(J) Bar graph showing tumor weight of orthotopically transplanted IL33 WT and IL33 KO PDAC tumors (n=5).

(K-Q) Frequency of T_H2, ILC2, T_{reg}, CD8, neutrophils, MDSC and B cells out of total $CD45^+$ cells in orthotopically transplanted IL33 WT and IL33 KO PDAC tumors and peripheral blood mononuclear cell (PBMC) (n=3-5).

Results are shown as mean ±SD. p-values were calculated using Student t-test. Individual p-values are indicated in the figures.

FIGURE S4

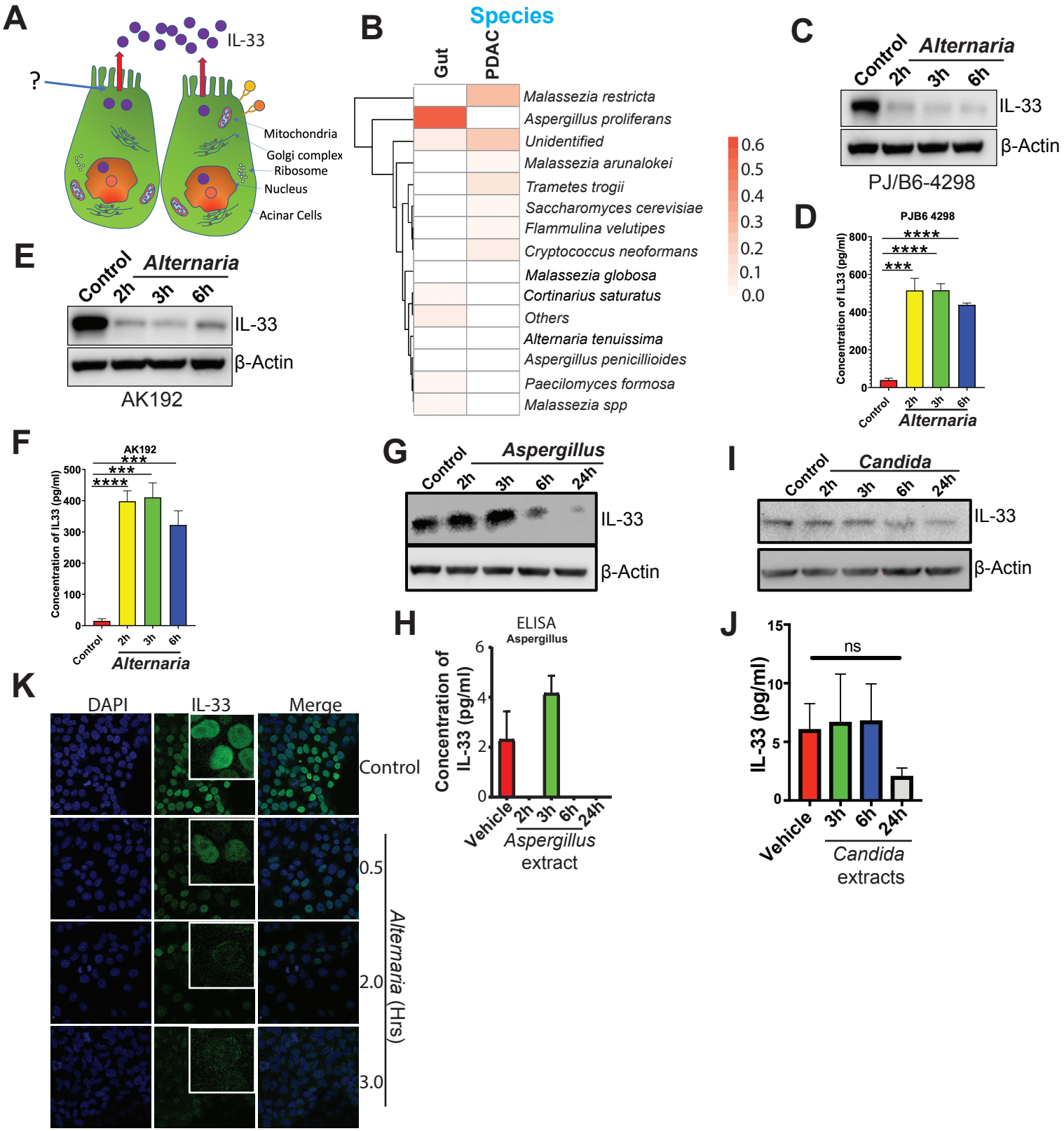
A
IL-33
?
Mitochondria
Golgi complex
Ribosome
Nucleus
Acinar Cells
B
Species
Gut
PDAC
Malassezia restricta
Aspergillus proliferans
Unidentified
Malassezia arunalokei
Trametes trogii
Saccharomyces cerevisiae
Flammulina velutipes
Cryptococcus neoformans
Malassezia globosa
Cortinarius saturatus
Others
Alternaria tenuissima
Aspergillus penicillioides
Paecilomyces formosa
Malassezia spp
0.6
0.5
0.4
0.3
0.2
0.1
0.0
C
Control
Alternaria
2h
3h
6h
IL-33
β-Actin
PJ/B6-4298
D
PJB6 4298
Concentration of IL33 (pg/ml)
****
****
***
Control
2h
3h
6h
Alternaria
E
Control
Alternaria
2h
3h
6h
IL-33
β-Actin
AK192
F
AK192
***
***
****
Concentration of IL33 (pg/ml)
Control
2h
3h
6h
Alternaria
G
Control
Aspergillus
2h
3h
6h
24h
IL-33
β-Actin
I
Control
Candida
2h
3h
6h
24h
IL-33
β-Actin
H
ELISA
Aspergillus
Concentration of IL-33 (pg/ml)
Vehicle
2h
3h
6h
24h
Aspergillus extract
J
ns
IL-33 (pg/ml)
Vehicle
3h
6h
24h
Candida extracts
K
DAPI
IL-33
Merge
Control
0.5
2.0
3.0
Alternaria (Hrs)

Figure S4: **Fungal mediated release of IL-33 from PDAC cell lines. Related to Figure 4.**

(A) Illustration showing the release of IL-33 from cancer cells and its unknown mechanism.

(B) The gut and intrapancreatic (n=6, biologically independent samples) mycobiomes of PDAC tumor bearing mice were analyzed by internal transcribed space (ITS) sequencing of 18S rRNA. The heatmap of relative abundance of the fungal species in gut vs PDAC.

(C) and (E) Western blot analysis of IL-33 in a time course experiment with *Alternaria alternata* extract treatment in PDAC cell lines PJ/B6-4298 and AK192.

(D) and (F) IL-33 was quantified in the spent media using ELISA in PDAC cell line PJ/B6-4298 and AK192 upon *Alternaria alternata* extract treatment.

(G) Western blot analysis of IL-33 in a time course experiment with *Aspergillus* extract treatment in AK-B6 PDAC cell line.

(H) IL-33 was quantified in spent media using ELISA in AK-B6 PDAC cell line upon *Aspergillus* extract treatment.

(I) Western blot analysis of IL-33 in a time course experiment with *Candida* extract treatment in AK-B6 PDAC cell line.

(J) IL-33 was quantified in spent media using ELISA in AK-B6 PDAC cell line upon *Candida* extract treatment.

(K) Confocal images showing IL-33 release from AK-B6 PDAC cell line upon *Alternaria alternata* extract treatment. β-actin was used as a loading control for all the western blots. Results are shown as mean ±SD. p-values were calculated using Student t-test. Individual p-values are indicated in the figures.

FIGURE S5:

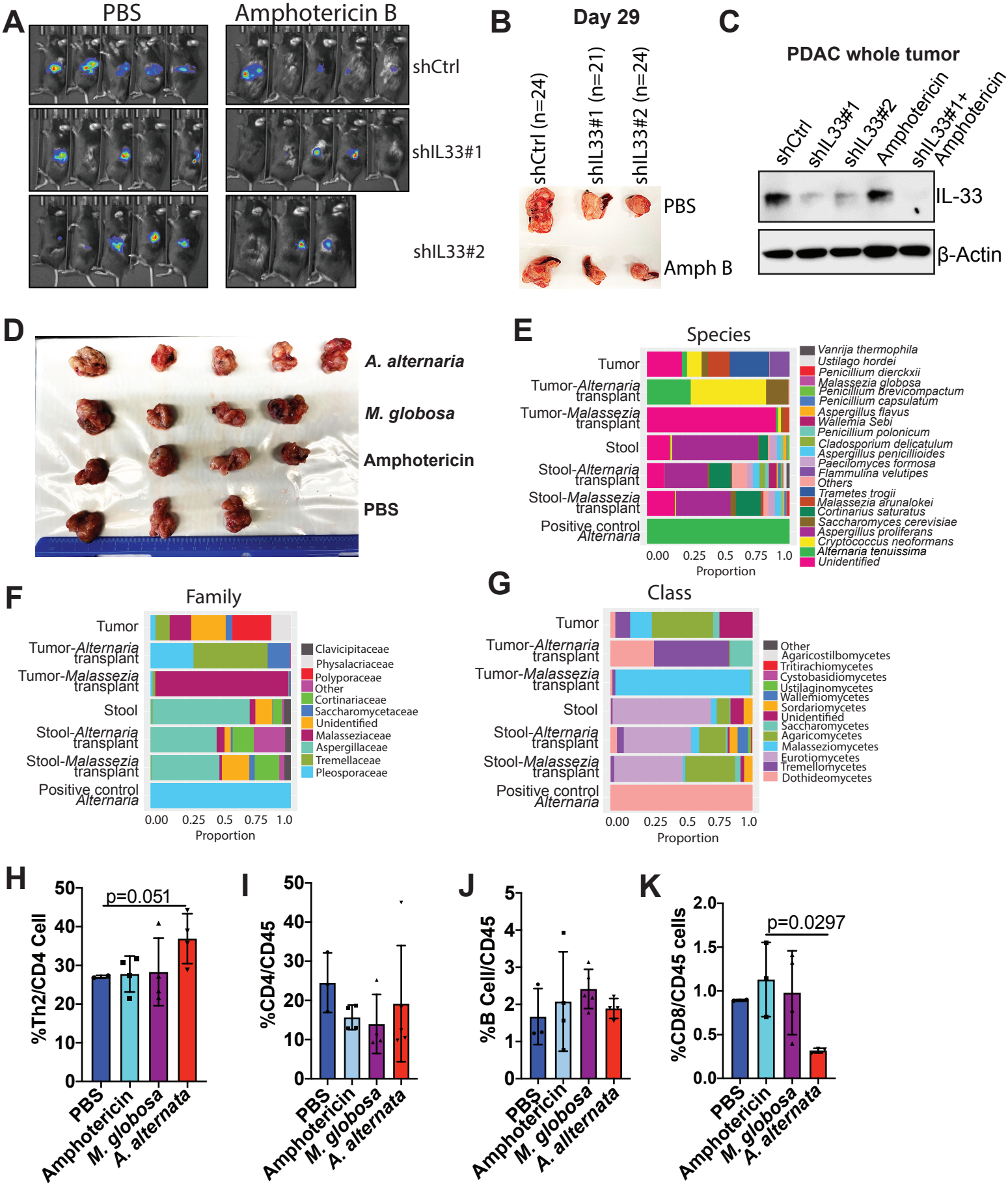
A
PBS
Amphotericin B
shCtrl
shIL33#1
shIL33#2
B
Day 29
shCtrl (n=24)
shIL33#1 (n=21)
shIL33#2 (n=24)
PBS
Amph B
C
PDAC whole tumor
shCtrl
shIL33#1
shIL33#2
Amphotericin
shIL33#1+ Amphotericin
IL-33
β-Actin
D
A. alternaria
M. globosa
Amphotericin
PBS
E
Species
Tumor
Tumor-Alternaria transplant
Tumor-Malassezia transplant
Stool
Stool-Alternaria transplant
Stool-Malassezia transplant
Positive control Alternaria
0.00 0.25 0.5 0.75 1.0
Proportion
Vanrija thermophila
Ustilago hordei
Penicillium dierckxii
Malassezia globosa
Penicillium brevicompactum
Penicillium capsulatum
Aspergillus flavus
Wallemia Sebi
Penicillium polonicum
Cladosporium delicatulum
Aspergillus penicillioides
Paecilomyces formosa
Flammulina velutipes
Others
Trametes trogii
Malassezia arunalokei
Cortinarius saturatus
Saccharomyces cerevisiae
Aspergillus proliferans
Cryptococcus neoformans
Alternaria tenuissima
Unidentified
F
Family
Tumor
Tumor-Alternaria transplant
Tumor-Malassezia transplant
Stool
Stool-Alternaria transplant
Stool-Malassezia transplant
Positive control Alternaria
0.00 0.25 0.5 0.75 1.0
Proportion
Clavicipitaceae
Physalacriaceae
Polyporaceae
Other
Cortinariaceae
Saccharomycetaceae
Unidentified
Malasseziaceae
Aspergillaceae
Tremellaceae
Pleosporaceae
G
Class
Tumor
Tumor-Alternaria transplant
Tumor-Malassezia transplant
Stool
Stool-Alternaria transplant
Stool-Malassezia transplant
Positive control Alternaria
0.00 0.25 0.5 0.75 1.0
Proportion
Other
Agaricostilbomycetes
Tritirachiomycetes
Cystobasidiomycetes
Ustilaginomycetes
Wallemiomycetes
Sordariomycetes
Unidentified
Saccharomycetes
Agaricomycetes
Malasseziomycetes
Eurotiomycetes
Tremellomycetes
Dothideomycetes
H
%Th2/CD4 Cell
p=0.051
PBS
Amphotericin
M. globosa
A. alternata
I
%CD4/CD45
PBS
Amphotericin
M. globosa
A. alternata
J
%B Cell/CD45
PBS
Amphotericin
M. globosa
A. alltternata
K
%CD8/CD45 cells
p=0.0297
PBS
Amphotericin
M. globosa
A. alternata

Figure S5: **Mycobiome promotes PDAC tumor progression. Related to Figure 5.**

(A) Bioluminescence images showing orthotopically transplanted shCtrl and shIL33 (#1 and #2) PDAC isogenic mouse cell lines with or without amphotericin B treatment (n=5).

(B) Representative images of control (n=24) and shIL33 (#1 [n=21] and #2 [n=24]) orthotopically transplanted PDAC tumors with or without amphotericin B treatment. The *n* value is based on three independent experiments.

(C) Western blot analysis of IL-33 in orthotopically transplanted tumor lysate from shCtrl and shIL33 (#1 and #2) PDAC isogenic mouse cell lines with or without amphotericin B treatment.

(D) Gross image showing orthotopically transplanted isogenic mouse cell line tumors with or without fungal repopulation (n=5). Missing tumors are mice died of tumor burden.

(E), (F), and (G) 18S sequencing data showing gut and intratumor fungal abundancies as species, family and class.

(H), (I), (J) and (K) Frequency of T_H2 out of total $CD4^+$ cells, frequency of $CD4^+$T, B and $CD8^+$T cells in *Alternaria alternata* and *Malassezia globosa* rechallenge experiments after fungal depletion in orthotopically transplanted isogenic PDAC tumors mice (n=3-5). Results are shown as mean ±SD. p-values were calculated using Student t-test. Individual p-values are indicated in the figures.

FIGURE S6

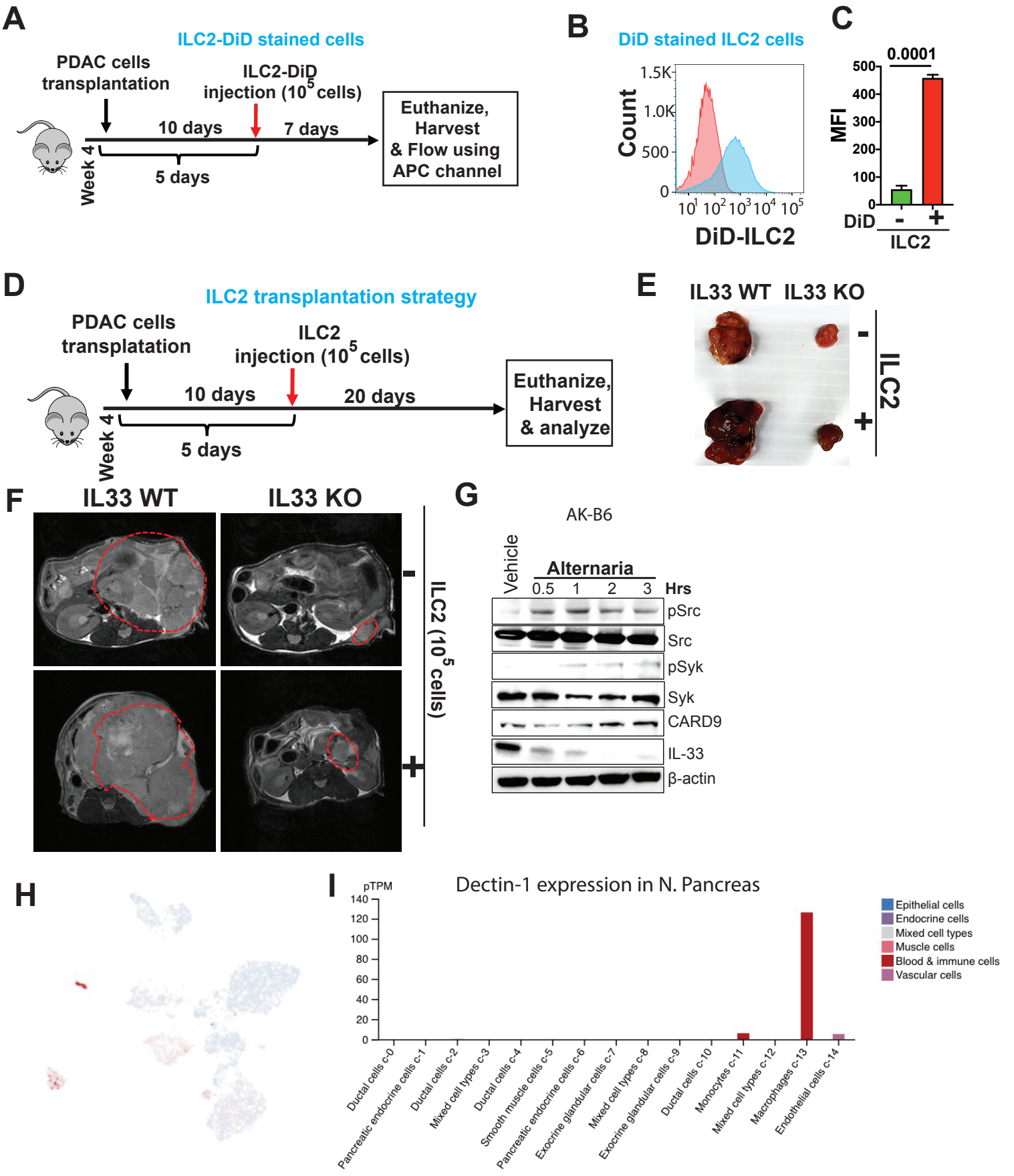
A
ILC2-DiD stained cells
PDAC cells transplantation
ILC2-DiD injection (10^5 cells)
10 days
7 days
Week 4
5 days
Euthanize, Harvest & Flow using APC channel
B
DiD stained ILC2 cells
Count
1.5K
1.0K
500
0
DiD-ILC2
C
0.0001
MFI
DiD
ILC2
D
ILC2 transplantation strategy
PDAC cells transplatation
ILC2 injection (10^5 cells)
10 days
20 days
Week 4
5 days
Euthanize, Harvest & analyze
E
IL33 WT
IL33 KO
ILC2
F
IL33 WT
IL33 KO
ILC2 (10^5 cells)
G
AK-B6
Vehicle
Alternaria
0.5
1
2
3
Hrs
pSrc
Src
pSyk
Syk
CARD9
IL-33
β-actin
H
I
Dectin-1 expression in N. Pancreas
pTPM
Epithelial cells
Endocrine cells
Mixed cell types
Muscle cells
Blood & immune cells
Vascular cells
Ductal cells c-0
Pancreatic endocrine cells c-1
Ductal cells c-2
Mixed cell types c-3
Ductal cells c-4
Smooth muscle cells c-5
Pancreatic endocrine cells c-6
Exocrine glandular cells c-7
Mixed cell types c-8
Exocrine glandular cells c-9
Ductal cells c-10
Monocytes c-11
Mixed cell types c-12
Macrophages c-13
Endothelial cells c-14

Figure S6: **IL-33 mediated ILC2 recruitment is necessary for tumor progression. Related to Figure 6.**

(A) Schematic showing ILC2 adoptive transfer strategy. Four-week-old mice were transplanted with IL33 WT and IL33 KO PDAC cells. Ten days post transplantation, 10^5 ILC2 cells, labelled with DiD dye, were injected retro-orbitally and tumor progression was monitored.

(B) Representative histogram of control ILC2 cells (red histogram) and DiD labelled ILC2 cells (blue histogram) in PDAC tumor.

(C) Bar graph showing the mean fluorescence intensity (MFI) of control and DiD labelled ILC2 cells in PDAC tumor.

(D) Schematic showing ILC2 adoptive transfer strategy. Six-week-old mice were transplanted with IL33 WT and IL33 KO PDAC cells. Ten days post transplantation, $2X10^5$ ILC2 cells were injected retro-orbitally and tumor progression was monitored.

(E) Representative images of IL33 WT and IL33 KO PDAC tumor adoptively transferred with or without ILC2 cells (n=3).

(F) MRI scans showing axial images of IL33 WT and IL33 KO PDAC tumors, with or without ILC2 adoptive transfer.

(G) Western blot analysis of Src, p-Src, Syk, p-Syk, CARD9 and IL-33 in AK-B6 PDAC cell line, treated with *Alternaria* extract. β-actin was used as a loading control.

(H) and (I) Representative plots showing Dectin-1 expression in different cell types in normal human pancreas. Data was sourced from The Human Protein Atlas (Uhlen et al., 2017, Uhlen et al., 2015).

Results are shown as mean ±SD. p-values were calculated using Student t-test. Individual p-values are indicated in the figures.

Table S1: Oligonucleotide Sequences
Related to STAR METHODS

Related to	Name	Source	Oligonucleotide Sequences
RT-qPCR PRIMERS	*Il33*	IDT	TGAGACTCCGTTCTGGCCTC
			CTCTTCATGCTTGGTACCCGAT
	Tph1	IDT	CACGAGTGCAAGCCAAGGTTT
			AGTTTCCAGCCCCGACATCAG
	Il5	IDT	TCACCGAGCTCTGTTGACAA
			CCACACTTCTCTTTTTGGCG
	Il13	IDT	TGAGGAGCTGAGCAACATCACACA
			TGCGGTTACAGAGGCCATGCAATA
	Areg	IDT	GGTCTTAGGCTCAGGACATTA
			CGCTTATGGAAACCTCTC
	Actb	IDT	GGCTGTATTCCCCTCCATCG
			CCAGTTGGTAACAATGCCATGT
shRNA PRIMERS	TRCN0000173352 (IL33 5')	Sigma-Aldrich	CCGGGCATCCAAGGAACTTCACTTTCTC GAGAAAGTGAAGTTCCTTGGATGCTTTTTTG
	TRCN0000176387 (IL33 3')	Sigma-Aldrich	CCGGCCATAAGAAAGGAGACTAGTTCTCGA GAACTAGTCTCCTTTCTTATGGTTTTTTG
CRISPR PRIMERS	*Il33*	Synthego	5' AUAGUAGCGUAGCGUAGUAGCACC
			3' AUCUCUUCCUAGAAUCCCG
FISH PRIMERS	D223	Molecular Probe, Thermo Fisher Scientific	CCACCCACTTAGAGCTGC
FUNGAL 18S PRIMERS	*ITS1F*	IDT	CTTGGTCATTTAGAGGAAGTAA
	ITS2	IDT	GCTGCGTTCTTCATCGATGC